Electronic Supplementary Material (ESI) for Materials Chemistry Frontiers.
This journal is © the Partner Organisations 2021

Supporting Information for

Stable Two-Dimensional Lead Iodide Hybrid Materials for Light Detection and Broadband Photoluminescence

Mohamed Saber Lassoued,[a,b] Yuan-Chao Pang,[a,b] Qian-Wen Li,[a,b] Xinkai Ding,[b] Bo Jiao,[c,d] Hua Dong,[c,d] Guijiang Zhou,[a] Shujiang Ding,[a] Zhicheng Zhang,[a] Zhaoxin Wu,[c,d] Gaoyang Gou,[b,*] Zongyou Yin,[e] Ju Li[e] and Yan-Zhen Zheng*[a,b]

---

a School of Chemistry, Xi'an Key Laboratory of Sustainable Energy and Materials Chemistry, MOE Key Laboratory for Nonequilibrium Synthesis and Modulation of Condensed Matter, Xi'an Jiaotong University, Xi'an 710049 China. E-mail: zheng.yanzhen@xjtu.edu.cn

b Frontier Institute of Science and Technology (FIST), State Key Laboratory for Mechanical Behavior of Materials, and School of Physics, Xi'an Jiaotong University, Xi'an 710054, China. E-mail: gougaoyang@xjtu.edu.cn

c Key Laboratory of Photonics Technology for Information, Key Laboratory for Physical Electronics and Devices of the Ministry of Education, Department of Electronic Science and Technology, School of Electronic and Information Engineering, Xi'an Jiaotong University, Xi'an 710049, China.

d Collaborative Innovation Center of Extreme Optics, Shanxi University, Taiyuan 030006, China.

e Department of Nuclear Science and Engineering, Department of Materials Science and Engineering, Massachu-setts Institute of Technology, Cambridge, MA 02139, United States.

Table of Contents

1. Experimental Section

1.1. General remarks

Single crystal X-ray diffraction data of **1Pb** and **2Pb** were collected on a Bruker SMART APEX II CCD diffractometer with graphite monochromated Mo-k radiation (λ= 0.71073 Å) by using the θ-ω scan technique at 298 K. PXRD intensities were measured at ambient temperature (298 K) on a Rigaku D/max-IIIA diffractometer (Cu-kλ, λ=1.54056 Å). The crystalline powder samples were prepared by grinding the single-crystals and collected in the 2θ range of 5°–50° with a step size of 10°/min. Scanning electron microscopy (SEM) was performed using KYKY-EM3200, 25 KV instrument. Solid-state UV-Vis diffusion reflectance spectra of pressed powder and films samples were measured on a SHIMADZU UV-3600 UV-Vis-NIR spectrophotometer using $BaSO_4$ powder as the reflectance reference. All density-functional theory (DFT) calculations were carried out within the Vienna Ab initio Simulation Package (VASP). Room-temperature steady-state emission spectra were collected on powder samples using an Edinburgh FLS980 spectrofluorometer upon 450 nm excitation. The PLQY was achieved by incorporating an integrating sphere into the FLS980 spectrofluorometer. TGA experiments were performed on a TGA-50 (SHIMADZU) thermogravimetric analyzer in temperature range between 30° and 600°.

2. Materials and Sample Preparation

2.1. Materials

Chemicals listed were used as purchased and without further purification: (i) Triethylenetetramine (TETA), 97%, sigma Aldrich; (ii) Potassium iodide, 99.995%, sigma Aldrich; (iii) Acetonitrile, 99%, sigma Aldrich; (iv) hydroiodic acid, 57% w/w, sigma Aldrich; (v) Lead (II) nitrate, 99%, sigma Aldrich.

2.2. Preparation of 1Pb and 2Pb Single crystals

Crystals of **1Pb**: A mixture of $Pb(NO_3)_2$ (0.331 g, 1 mmol), HI (1 mmol), TETA (0.5 mmol), and KI (0.166 g, 1 mmol) were dissolved in 10ml mixed solvent (H_2O : CH_3CN = 8 : 2), stirred in the air for 10 minutes before transferred to a 15 mL Teflon-lined auto-clave and heated at 130°C for 24 hrs. The reactants were then cooled to room temperature in a rate of 5°C / h to obtain Luminous yellow needle-like crystals. (Yield: ca. 40% based on Pb). XRD indicates the phase purity (**Figure S1a**).

Crystals of **2Pb**: A mixture of $Pb(NO_3)_2$ (0.331 g, 1 mmol), HI (2 mmol), TETA (1 mmol), and KI (0.332 g, 2 mmol) were dissolved in 10 ml deionized water, stirred in the air for 10 minutes before transferred to a 15 mL Teflon-lined auto-clave and heated at 150°C for 48 hrs. The reactants were then cooled to room temperature in a rate of 5 °C / h to obtain Luminous yellow rod-like crystals. (Yield: ca. 32% based on Pb). XRD indicates the phase purity (**Figure S1b**).

2.3. Fabrication of 1Pb and 2Pb Films

Indium tin oxide coated glass (ITO) substrates were cleaned thoroughly and sequentially with commercial detergent in soapy water, deionized water, KOH solution, deionized water, and in a sonication bath. The substrates were then treated by UV–ozone treatment for 20 min prior before use. **1Pb** and **2Pb** organic-inorganic hybrid compounds (0.2 g for each compound) were dissolved in 1 mL of dimethylformamide solution (DMF) and were coated onto ITO glass substrate by spin coating method at 1000 rpm for 60 second. To evaporate the residual solvent, the obtained film was followed by annealing on a hot plate at 80 °C for 10 minutes.

3. Characterization methods and Simulation details

3.1. Characterization methods

X-ray Crystallographic Study

Single-crystal X-ray diffraction data collections for **1Pb** and **2Pb** were conducted on a Bruker SMART APEX II CCD diffractometer (Mo, λ = 0.71073 Å) by using the θ-ω scan technique at 298 K. The structures were solved by direct methods and refined with a full-matrix least-squares technique within the SHELXTL program package and Olex. [1, 2] All non-hydrogen atoms were refined anisotropically. The crystallographic details are provided in **Table S1-S5**. The crystallographic data for above compounds can be found in the Supporting Information or can be obtained free of charge from the Cambridge Crystallographic Data Centre via http://www.ccdc.cam.ac.uk/data_request/cif. CCDC Numbers: 2107024 (1Pb) and 2107027 (2Pb).

Optical absorption measurement. Solid-state UV-Vis diffusion reflectance spectra were measured at room temperature on a SHIMADZU UV-3600 UV-Vis-NIR spectrophotometer using $BaSO_4$ powder as the reflectance reference. The absorption spectra were calculated from reflectance spectra by the Kubelka-Munk function: $F(R) = \alpha/S = (1-R)^2/2R$, where R, α, and S are the coefficients for the reflection, the absorption and the scattering, respectively.

Photo response measurement During the photocurrent tests, a three-electrode system (a sample coated 0.5 × 0.5 cm ITO glass plate as the working electrode, and Ag/AgCl as the counter and reference electrodes) was used, and Na_2SO_4 (50 mL, 0.2 mol L^{-1}) was utilized as the supporting electrolyte solution. Photoresponse of the photodetector was measured using Keithley 2450 source meter under the illumination from a 350 W Xenon lamp irradiation . The lamp was kept on continuously, and a manual shutter was used to block exposure of the sample to the light. The sample was typically irradiated at intervals of 80 s.

The on/off ratio of the photodetector is calculated using equation **1**.

$$\frac{ON}{OFF} = \frac{I_{Light}}{I_{dark}} \quad (1)$$

Where I_{light} is the photocurrent (636 nA for **1Pb** and 780 nA for **2Pb** and I_{dark} is the dark current (20 nA and 42 nA for **1Pb** and **2Pb** respectively).

The responsivity is obtained using the following equation **2**.

$$R = \frac{I_{light} - I_{dark}}{P_0 S} \quad (2)$$

where P_0 is the intensity of light (0.35 W/cm^2) and S is the area of the device (0.25 cm^2). The detectivity (D*) and the external quantum efficiency (EQE) were calculated using the following equations **3** and **4**.

$$D^* = RS^{\frac{1}{2}}/(2eI_d)^{\frac{1}{2}} \quad (3)$$

$$EQE = R * \frac{12408}{\lambda} \quad (4)$$

Where R is the responsivity , S is the effective area of light irradiation , e is the electronic charge , Id is the dark current, λ is the wavelength of irradiation.

Stability studies. Freshly prepared films of **1Pb** and **2Pb** were stored either in the dark to minimize light exposure and the relative humidity was maintained at ~55% humidity for 7 days. Freshly prepared films of **1Pb** and **2Pb** were exposed to UV light for 24 hours at room temperature.

3.2 Simulation details Computational methods. The crystallographic data of compound **1Pb** and **2Pb** obtained from Single Crystal XRD tests were used to calculate the electronic band

structures and densities of the states (DOS). All the calculations in this work were carried out using density functional theory (DFT) as implemented in the Vienna Ab initio Simulation Package (VASP). The generalized gradient approximation (GGA) Perdew−Burke−Ernzerhof (PBE) functional was used for electronic structure calculations. [3,4] The projector augmented wave (PAW) method was applied to treat the electron–core interactions. [5] The cutoff energy for plane waves was set to 550 eV and the Brillouin zone was sampled by a 5×2×3 mesh for **1Pb** and a 4×4×2 mesh for **2Pb**.

4. Supporting Tables and Figures

Table S1 Summary of crystal data and structural refinements of **1Pb** and **2Pb**

	1Pb	**2Pb**
Empirical formula	$C_6 H_{18} I_6 N_4 Pb_3$	$C_6 H_{18} I_8 N_4 Pb_4$
Formula weight	1529.25	1990.25
Crystal dimensions (mm)	0.11*0.22*0.15	0.13*0.19*0.14
Crystal system	Monoclinic	Monoclinic
Space group	$P2_1/c$	C2/c
a/Å	8.8484(8)	24.937(4)
b/Å	19.3860(18)	9.1908(14)
c/Å	15.5239(11)	26.522(4)
α/°	90	90
β/°	115.255(4)	94.213(2)
γ/°	90	90
Volume/Å^3	2408.4(4)	6062.2(16)
Z	4	8
ρ calcg/cm^3	4.218	4.361
μ /mm^{-1}	28.606	30.299
F(000)	2584.0	6672.0
Index ranges	-11<=h<=11, -25<=k<=25, -20<=l<=20	-32<=h<=32, -11<=k<=11, -34<=l<=34
Data Completeness	99.5%	96.6%
Data/restraints/parameters	5536/7/172	6849/2/199
Goodness-of-fit on F2	1.19	1.025
Weight	$w = 1/[\sigma^2(Fo^2) + (0.000P)^2 + 274.3427P]$ where $P = (Fo^2 + 2Fc^2)/3$	$w = 1/[\sigma^2(Fo^2) + (0.1086P)^2 + 497.4207P]$ where $P = (Fo^2 + 2Fc^2)/3$
$R=\sum\|\|Fo-Fc\|\|/\sum\|Fo\|$,$wR_2$	$R_1 = 0.0435$, $wR_2 = 0.1225$	R1 = 0.0670, wR2 = 0.192

$R1 = \Sigma||Fo| - |Fc||/\Sigma|Fo|$, $wR_2 = [\Sigma w(Fo^2 - Fc^2)^2 / \Sigma w(Fo^2)^2]^{1/2}$

Table S2 Summary of selected bond lengths (Å) and bond angles (°) of **1Pb**

Bond	Lengths/Å	Bond pair	Angles / °	Bond pair	Angles / °
Pb1—N1	2.447 (15)	N1—Pb1—N3	99.4 (5)	I2—Pb3—I5^{iii}	105.96 (3)
Pb1—N3	2.528 (15)	N1—Pb1—N4	80.0 (6)	I2—Pb3—I6	99.85 (4)
Pb1—N4	2.628 (17)	N1—Pb1—N2	70.0 (7)	Pb2—I3—Pb3^{ii}	94.89 (3)
Pb1—N2	2.548 (17)	N3—Pb1—N4	69.4 (6)	Pb3—I3—Pb2	89.77 (3)
Pb2—I3	3.3028 (12)	N3—Pb1—N2	68.6 (6)	Pb3—I3—Pb3^{ii}	95.22 (3)
Pb2—I1^{i}	3.3314 (13)	N2—Pb1—N4	122.4 (6)	Pb2^{iii}—I1—Pb2^{ii}	92.69 (3)
Pb2—I5	3.1494 (13)	I3—Pb2—I1^{ii}	82.95 (3)	Pb3—I1—Pb2 ^{iii}	84.08 (3)
Pb2—I4	3.0447 (13)	I3—Pb2—I1i	80.41 (3)	Pb3—I1—Pb2^{ii}	96.79 (3)
Pb2—I6	3.1122 (14)	I1^{i}—Pb2—I1^{ii}	87.31 (3)	Pb2—I5—Pb3^{i}	84.64 (3)
Pb3—I3	3.1099 (12)	I5—Pb2—I3	170.10 (3)	Pb2—I6—Pb3	90.75 (3)
Pb3—I3^{ii}	3.3673 (12)	I5—Pb2—I1^{ii}	87.98 (3)	C5—N1—Pb1	113.7 (15)
Pb3—I1	3.1806 (13)	I5—Pb2—I1^{i}	95.25 (3)	C1—N3—Pb1	113.7 (11)
Pb3—I6	3.2474 (13)	I4—Pb2—I3	98.33 (3)	C6—N2—Pb1	117.3 (17)
Pb3—I2	3.1140 (13)	I4—Pb2—I1^{i}	95.26 (3)	N3—C5—C6	108.9 (14)
N1—C5	1.46 (4)	I4—Pb2—I1^{ii}	177.28 (4)	C6—N2—C2	117.2 (17)
N3—C1	1.50 (2)	I4—Pb2—I5	90.89 (3)	N3—C1—C3	110.7 (15)
N3—C4	1.41 (3)	I4—Pb2—I6	87.10 (4)	N2—C2—C5	113.8 (18)
N4—C3	1.47 (3)	I4—Pb2—I3	88.68 (3)	N4—C3—C1	111.4 (17)
N2—C2	1.48 (3)	I3—Pb3—I3^{ii}	84.78 (3)	N3—C4—C6	112.0 (16)
N2—C6	1.43 (3)	I3—Pb3— I1	93.43 (3)	N1—C5—C2	109.1 (17)
C1—C3	1.513 (10)	I3—Pb3—I5^{iii}	162.51 (3)	N2—C6—C4	109.8 (19)
C2—C5	1.52 (4)	I3—Pb3—I6	89.72 (3)	I1—Pb3—I6	171.44 (4)
C4—C6	1.55 (3)	I3—Pb3—I2	89.72 (3)	I5^{iii}—Pb3—I3^{ii}	80.54 (3)
		I1—Pb3—I3^{ii}	85.14 (3)	I2—Pb3—I1	88.13 (3)
		I1—Pb3—I5 ^{iii}	94.75 (3)		

Symmetry codes: (i) x−1, y, z; (ii) −x+2, −y+1, −z+2; (iii) x+1, y, z

Table S3 Summary of selected bond lengths (Å) and bond angles (°) of **2Pb**

Bond	Lengths/Å	Bond pair	Angles / °	Bond pair	Angles / °
Pb1—I1	3.2300 (13)	I1^{i}—Pb1—I1	176.98 (3)	I8—Pb3—I4	92.80 (4)
Pb1—I1^{i}	3.1859 (13)	I1^{i}—Pb1—I2	88.35 (4)	I8—Pb3—I5	101.05 (4)
Pb1—I2	3.2243 (13)	I1^{i}—Pb1—I4	85.74 (3)	I8—Pb3—I7	91.74 (4)
Pb1—I2^{ii}	3.1785 (13)	I1—Pb1—I4	93.81 (3)	N2—Pb4—N1	68.6 (6)
Pb1—I4	3.2743 (14)	I1^{i}—Pb1—I7^{i}	92.40 (3)	N3—Pb4—N2	69.3 (5)
Pb1—I7^{i}	3.2045 (13)	I2^{ii}—Pb1—I1^{i}	88.62 (4)	N3—Pb4—N4	87.3 (6)
Pb2—I2	3.3768 (14)	I2—Pb1—I1	94.65 (4)	N3—Pb4—N1	107.0 (6)
Pb2—I3	3.1318 (13)	I2^{ii}—Pb1—I1	88.38 (4)	N4—Pb4—N2	120.8 (6)
Pb2—I4	3.3690 (14)	I2^{ii}—Pb1—I2	176.96 (3)	N4—Pb4—N1	68.0 (5)
Pb2—I5	3.0784 (14)	I2—Pb1—I4	91.55 (3)	Pb1^{ii}—I1—Pb1	91.51 (3)
Pb2—I6	3.0543 (14)	I2^{ii}—Pb1—I4	87.92 (3)	Pb1^{i}—I2—Pb2	93.10 (3)
Pb3—I3^{iii}	3.2140 (13)	I2^{ii}—Pb1—I7^{i}	91.70 (3)	Pb2—I3—Pb3^{iv}	94.97 (4)
Pb3—I4	3.2598 (14)	I7^{i}—Pb1—I4	178.11 (4)	Pb1—I4—Pb2	89.81 (3)
Pb3—I5	3.2451 (14)	I3—Pb2—I2	85.62 (3)	Pb3—I4—Pb1	90.01 (3)
Pb3—I7	3.2637 (14)	I3—Pb2—I4	167.99 (4)	Pb3—I4—Pb2	86.26 (4)
Pb3—I8	3.0070 (14)	I4—Pb2—I2	87.32 (3)	Pb2—I5—Pb3	91.54 (4)
Pb4—N2	2.588 (15)	I5—Pb2—I2	85.92 (3)	Pb1^{ii}—I7—Pb3	92.65 (3)
Pb4—N3	2.505 (15)	I5—Pb2—I3	98.62 (4)	N1—C2—C3	110.5 (19)
Pb4—N4	2.567 (17)	I5—Pb2—I4	90.55 (4)	N1—C1—C6	109.8 (18)
Pb4—N1	2.596 (19)	I6—Pb2—I2	169.29 (4)	C5—N2—Pb4	112.6 (12)
C2—C3	1.52 (3)	I6—Pb2—I3	88.67 (4)	C6—N2—Pb4	110.9 (13)
C2—N1	1.51 (2)	I6—Pb2—I4	99.77 (4)	C6—N2—C5	111.5 (17)
C1—C6	1.52 (3)	I6—Pb2—I5	85.99 (4)	N2—C5—C4	107.7 (19)
N2—C5	1.50 (3)	I3^{iii}—Pb3—I4	170.46 (4)	C4—N3—Pb4	110.0 (12)
N2—C6	1.47 (3)	I3^{iii}—Pb3—I5	87.99 (4)	N4—C3—C2	110 (2)
C5—C4	1.517 (10)	I3^{iii}—Pb3—I7	88.86 (3)	N2—C6—C1	113.6 (16)
N3—C4	1.466 (10)	I4—Pb3—I7	91.42 (4)	C1—N1—C2	112.9 (17)
C3—N4	1.46 (3)	I5—Pb3—I4	89.64 (3)	C1—N1—Pb4	112.9 (13)
		I5—Pb3—I7	167.10 (4)	C2—N1—Pb4	113.0 (12

Symmetry codes: (i) −x+1/2, y−1/2, −z+1/2; (ii) −x+1/2, y+1/2, −z+1/2; (iii) x, y+1, z; (iv) x, y−1, z

Table S4 Potential hydrogen bonding data of compound **1Pb**

D-H	d(D-H)	d(H···A)	<DHA	d(D···A)	A	
N1-H1A	0.900	2.919	153.44	3.746	I1	[x-1, y, z]
N1-H1B	0.900	2.767	159.12	3.622	I6	[-x+1, y-1/2, -z+3/2]
N3-H3	0.910	2.934	153.43	3.770	I5	[-x, -y+1, -z+1]
N4-H4A	0.860	2.422	167.03	3.266	N1	
N2-H2	0.910	3.294	118.48	3.813	I4	

Table S5 Potential hydrogen data of compound **2Pb**

D-H	d(D-H)	d(H···A)	<DHA	d(D···A)	A	
C2-H2B	0.970	3.279	125.11	3.918	I2	[x+1/2, y+1/2, z]
N2-H2	0.980	3.249	154.56	4.155	I8	[x+1, y-1, z]
N3-H3A	0.890	2.890	163.88	3.753	I1	[x+1/2, y-1/2, z]
N3-H3B	0.890	3.261	122.67	3.816	I3	[-x+1, -y+1, -z]
N4-H4A	0.890	3.085	123.68	3.654	I3	[-x+1, -y+1, -z]
N4-H4A	0.890	3.167	144.59	3.926	I5	[-x+1, -y+2, -z]
N4-H4B	0.890	3.276	119.21	3.791	I3	[x+1/2, y+1/2, z]
C4-H4C	0.970	3.260	131.11	3.966	I6	[-x+1, -y+1, -z]
C4-H4D	0.970	2.983	172.14	3.946	I2	[x+1/2, y-1/2, z]
C6-H6A	0.970	3.178	128.22	3.855	I6	[x+1, y, z]
N1-H1	0.980	3.080	146.99	3.938	I8	[x+1, y, z]

Table S6 Photophysical properties of reported haloplumbate-based hybrids

Compds	λex (nm)	λem (nm)	CIE	τ(ns)	Ref
$[H_2BPP]Pb_2Br_6$	394	524	(0.38, 0.48)	16.57	[6]
$[H_2BPP]Pb_2Cl_6$	389	538	(0.33, 0.50)	2.7	[6]
NPM $_2Pb_3Br_{10}$	365	447/538	(0.33, 0.44)	4.21	[7]
(γ-MPAPB)	365	399/417/470	(0.22, 0.23)	2.52	[8]
$[(Pb_4Cl_2)\ (ndc)_4{\cdot}A_2]_n$	365	388	(0.25, 0.22)	0.73	[9]
$[(Pb_4Br_2)\ (ndc)_4{\cdot}A_2]_n$	365	393/684	(0.34, 0.29)	0.73	[9]
$[(Pb_4I_2)\ (ndc)_4{\cdot}A_2]_n$	365	390/684	(0.33, 0.28)	0.91	[9]

$[H_2BPP]$: 1,3-bis(4-pyridyl)-propane / NPM : N-propyl-morpholine / γ-MPAPB : γ-methoxy propyl amine)2PbBr4/ ndc : naphthalene dicarboxylate ; A : $(CH_3)_3NH^+$ and $(CH_3)_2NH_2{}^+$

Table S7 Comparaison of photodetectors performances for **1Pb** and **2Pb** with others reported systems

Compounds	D	Voltage (V)	I_{light} (nA)	R (μA/W)	D (Jones)	EQE (%)	Ref
1Pb	2D	0.7	636	7.04	$6.4*10^6$	2.39	This work
2Pb	2D	0.7	780	8.457	$7.7*10^6$	2.87	This work
PDBI	0D	1	194	1.14	$1.9*10^6$	0.4	[10]
$\{(Pb_4Cl_2)(ndc)_4{\cdot}[(CH_3)_3NH]_2\}_n$	1D	-	380	-	-	-	[9]
$\{[Pb(cbpy)_2](I_3)_4{\cdot}I_2\}_n$	2D	0.5	2600	-	-	-	[11]
$MAPbI_3$	3D	3	-	$3.49*10^6$	-	$1.19*10^3$	[12]
$(C_4H_9NH_3)_2PbBr_4$	2D	0.5	-	$2.1*10^8$	-	-	[12]
$(I\text{-}BA)_2(MA)_2Pb_3I_{10}$	2D	30	1000	12.78	-	-	[13]
Boron	2D	0	-	91.7	$1.6*10^8$	-	[14]
Cs_3BiBr_6	0D	6	-	25	$6*10^8$	0.008	[15]
$Cs_2AgBiBr_6$	3D	5	-	900	10^9	-	[16]

PDBI: $(1,3\text{-propanediammonium})_2Bi_2I_{10}{\cdot}2H_2O$ / ndc: naphthalene dicarboxylate / cbpy: 1-(3-carboxybenzyl)-4,4′-bipyridinium / MA: methylammonium / BA: butylammonium.

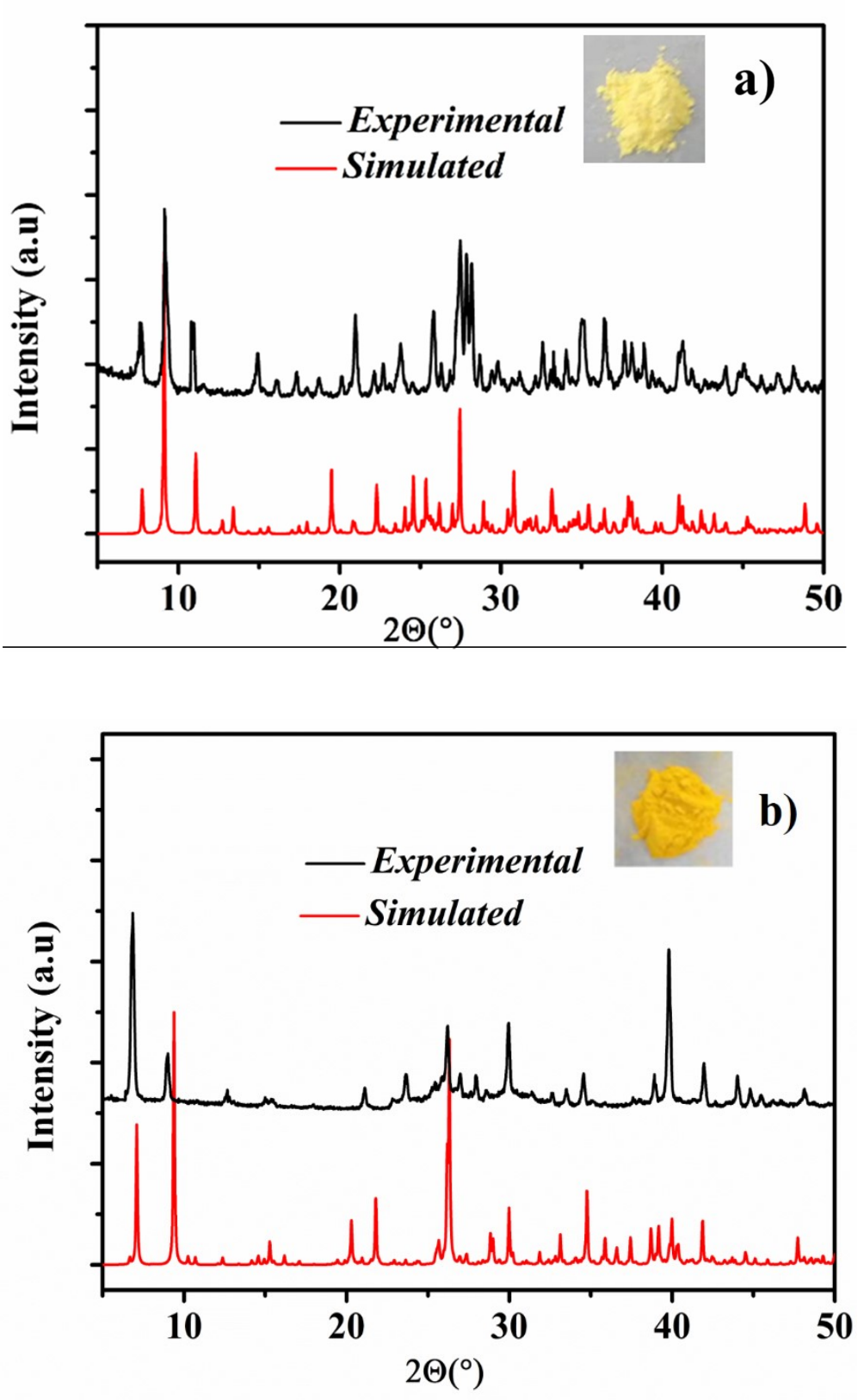

Figure S1. (a) Powder XRD patterns of **1Pb**. (b) Powder XRD patterns of **2Pb**.

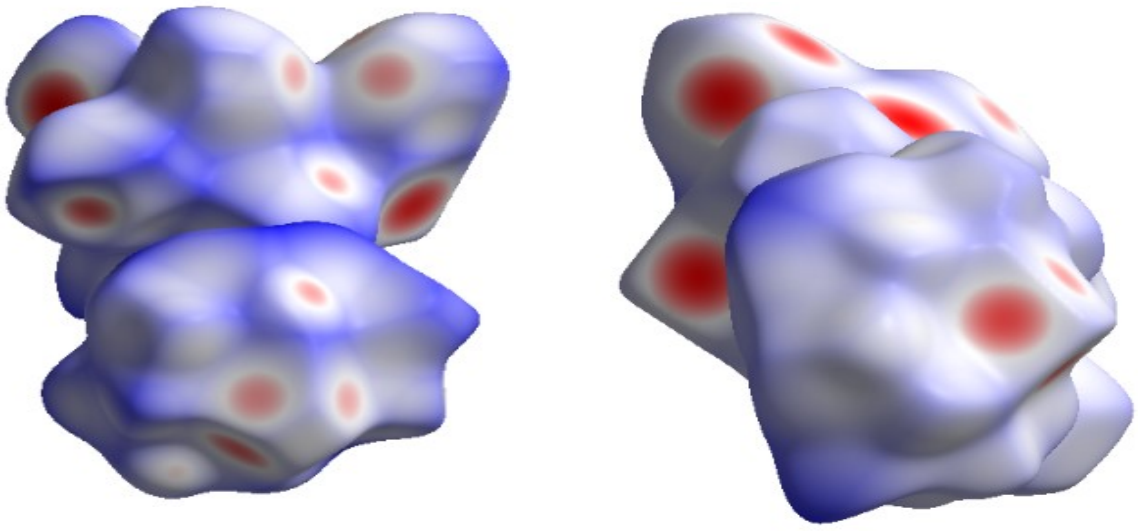

1Pb **2Pb**

Figure S2. Hirshfeld surfaces mapped with dnorm **1Pb** (a) and (b) **2Pb** (color coding: white, distance d equals VDW distance; blue, d exceeds VDW distance, red, d, smaller than VDW distance).

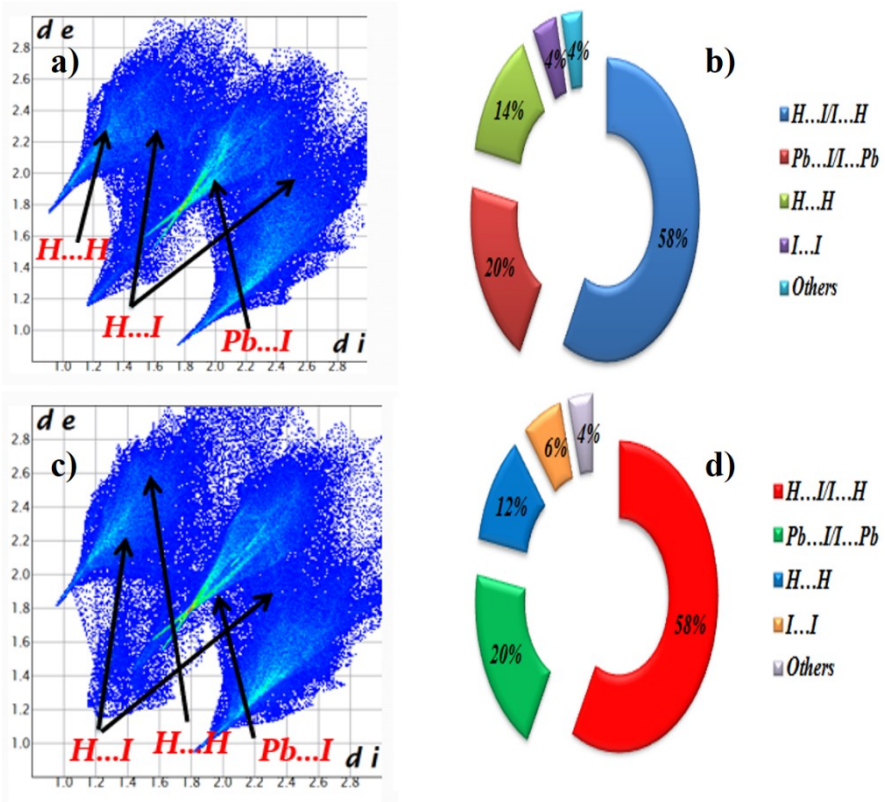

Figure S3. Two-dimensional finger print plots of **1Pb** (a) and **2Pb** (c). The population of close contact of **1Pb** (b) and **2Pb** (d) in crystal stacking.

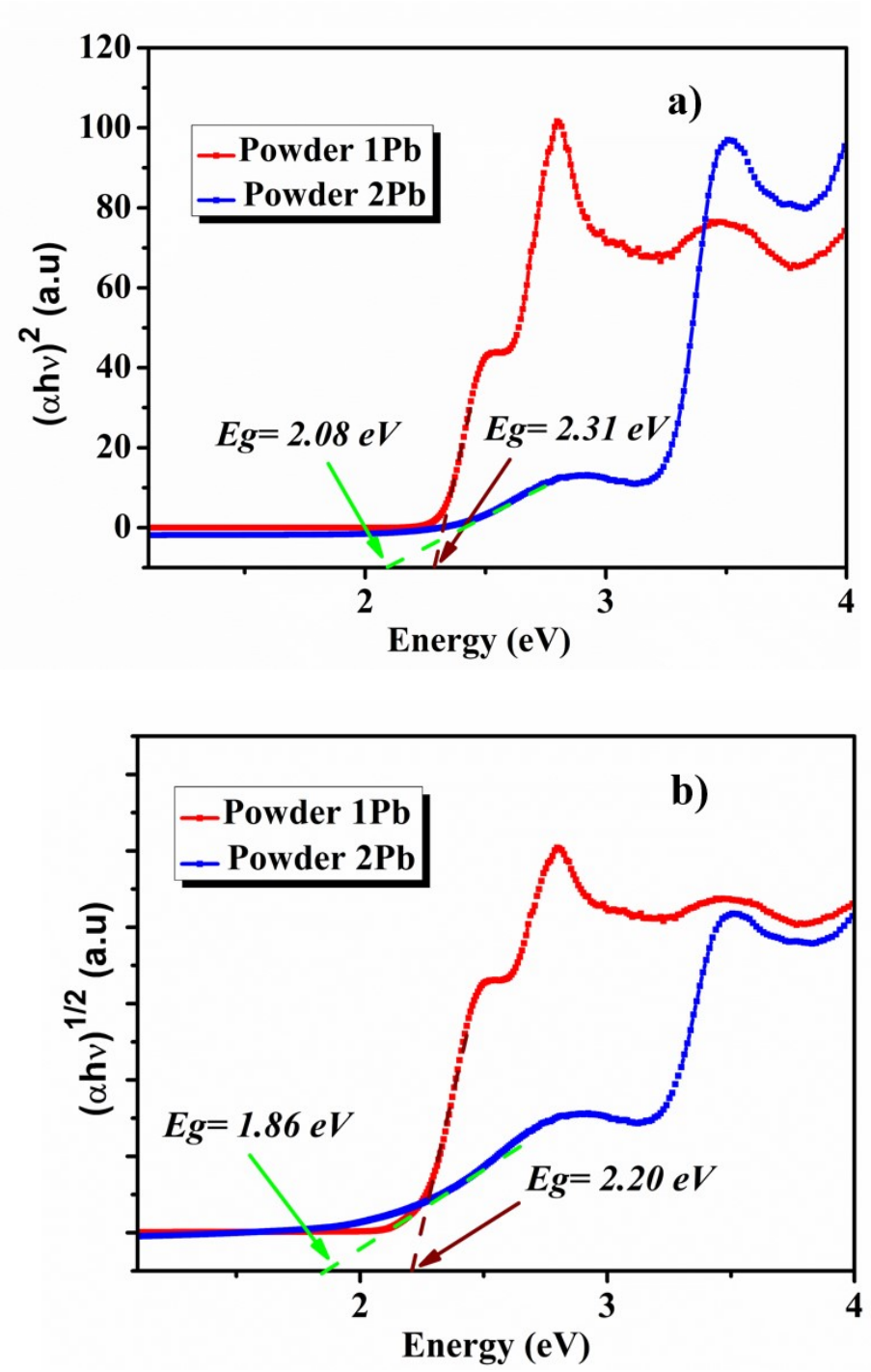

Figure S4. The Tauc Plot for a direct band gap (a) and for indirect band gap (b) semiconductor of **1Pb** and **2Pb**.

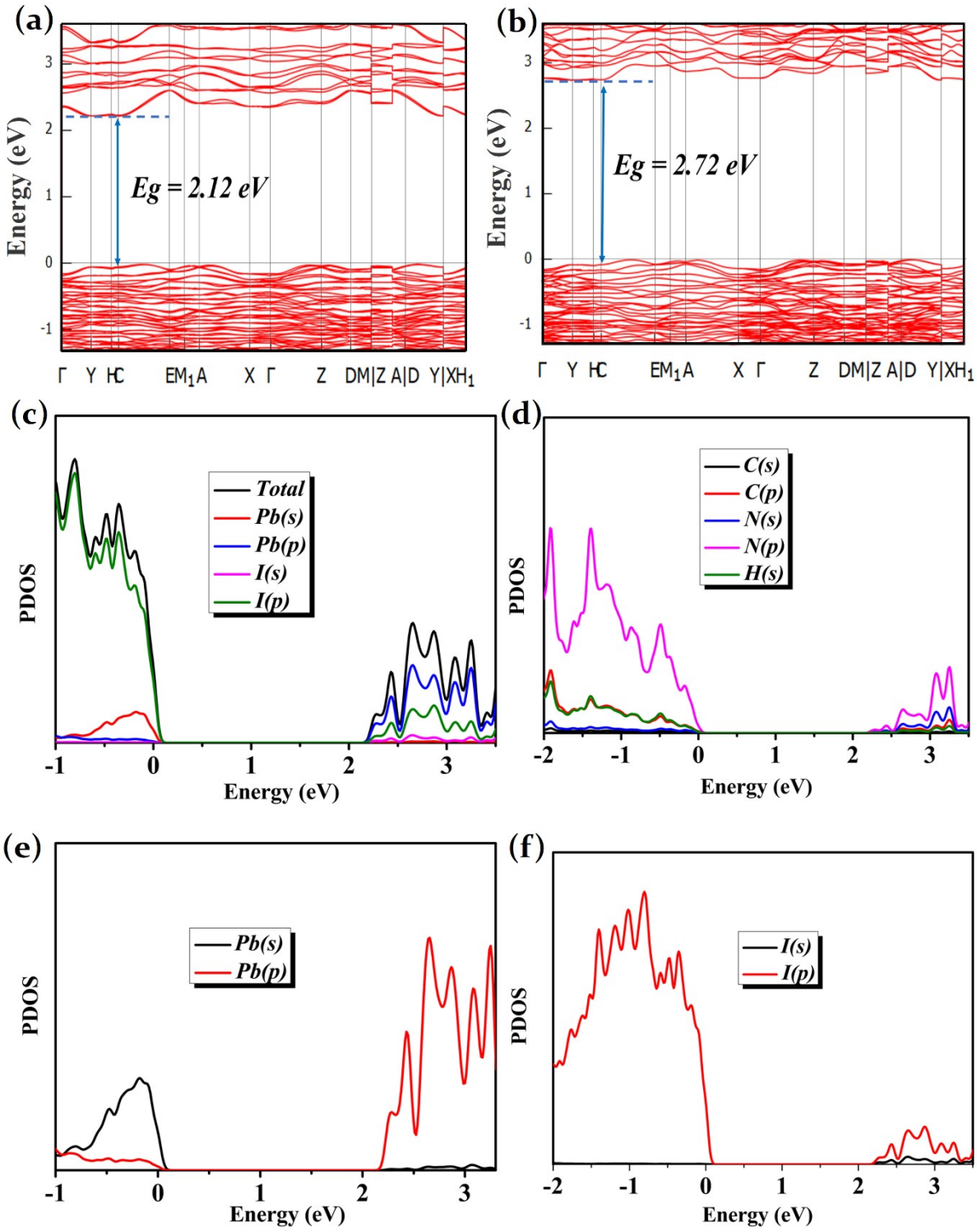

Figure S5. (a) Band structure of **1Pb** with SOC. (b) Band structure of **1Pb** without SOC. (c-f) Partial density of states (PDOS) of compound **1Pb** (inorganic part, organic part, Pb-s, Pb-p, and I-s, I-p).

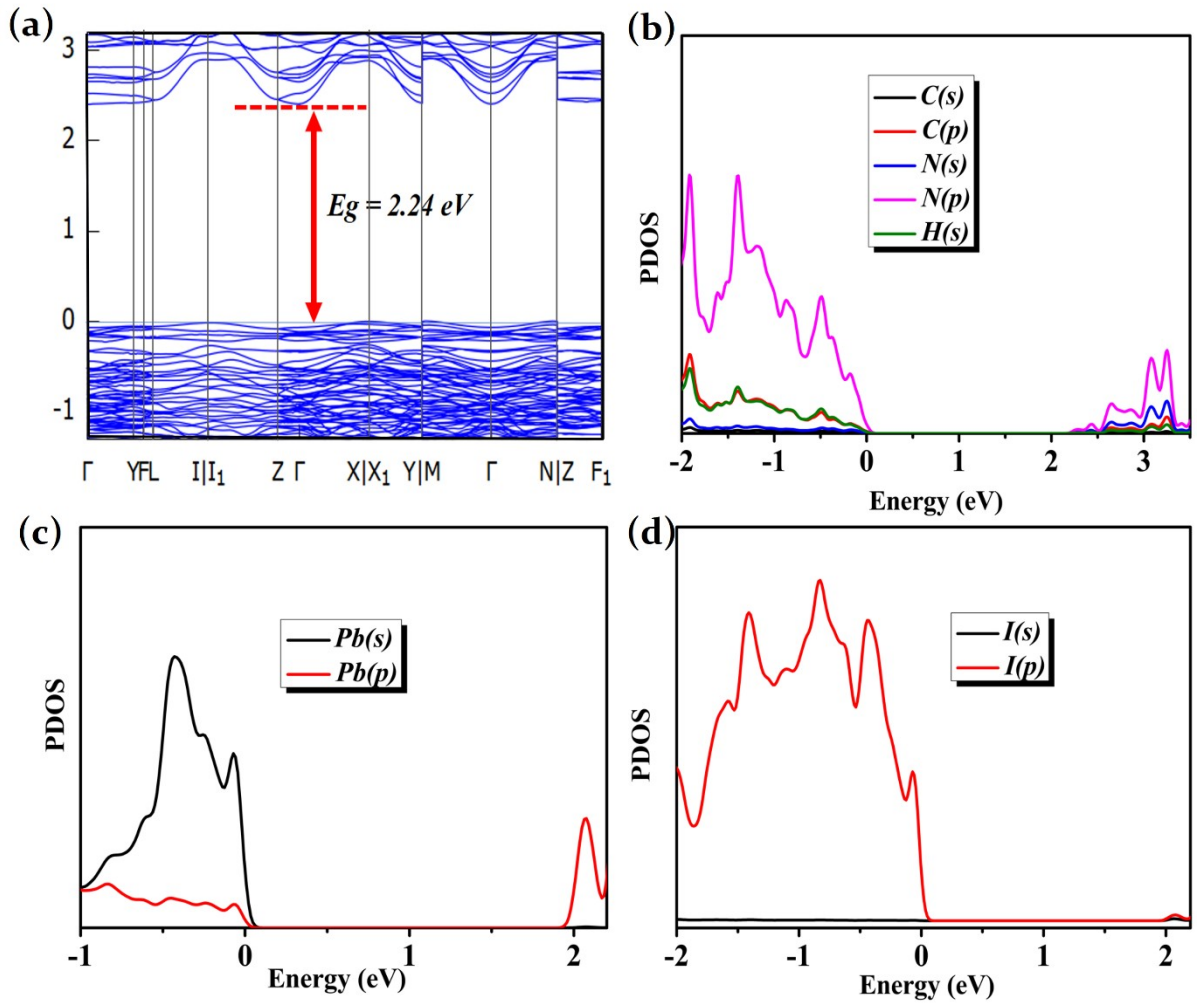

Figure S6. (a) Band structure of **2Pb** without SOC. (b-d) Partial density of states (PDOS) of compound **2Pb** (organic part, Pb-s, Pb-p, Pb-d and I-s, I-p).

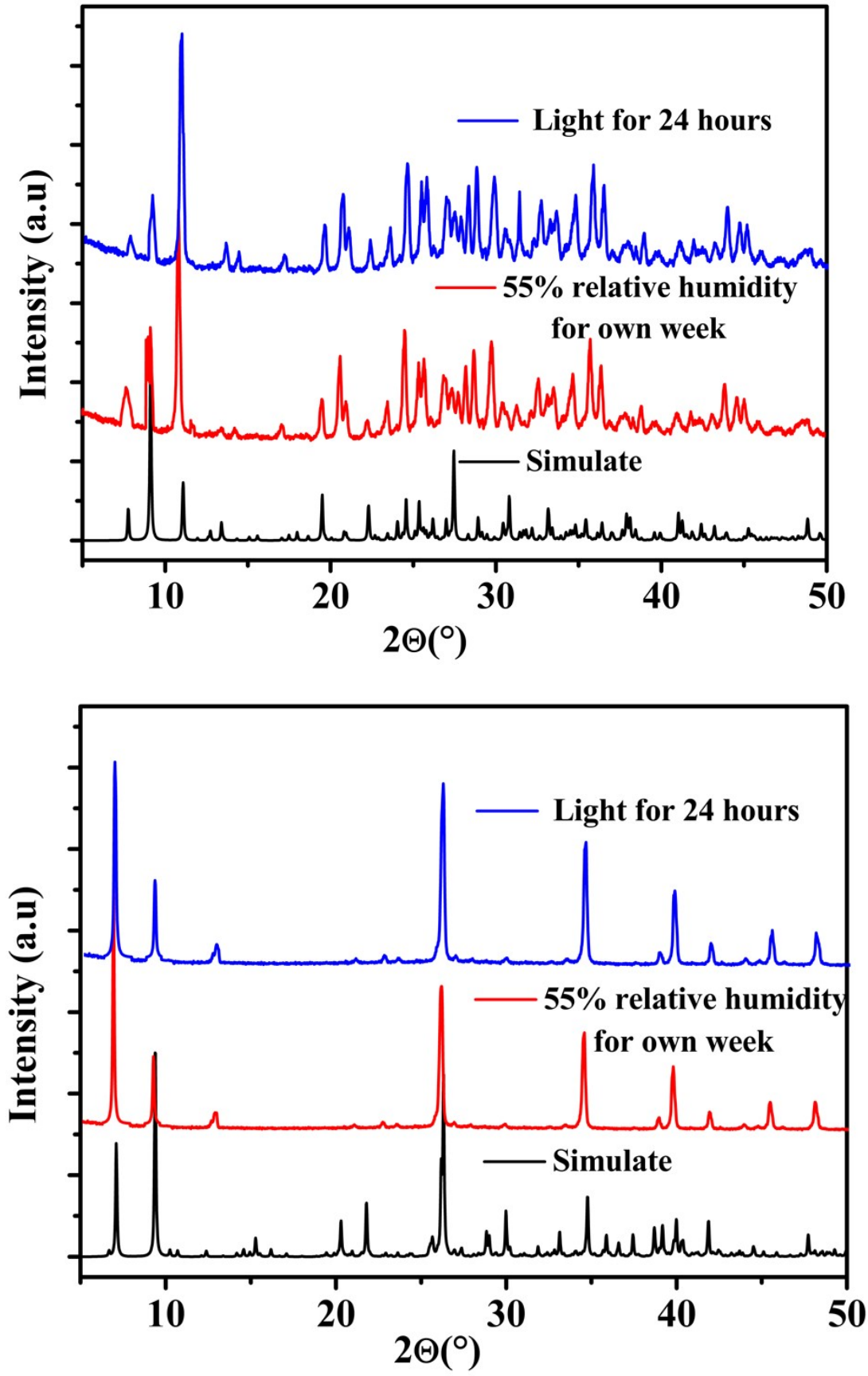

Figure S7. XRD patterns of **1Pb** (a) and **2Pb** (b) thin films after storage in ambient temperature for 7 days (relative humidity of 55%) and after exposing to light for 24 hours.

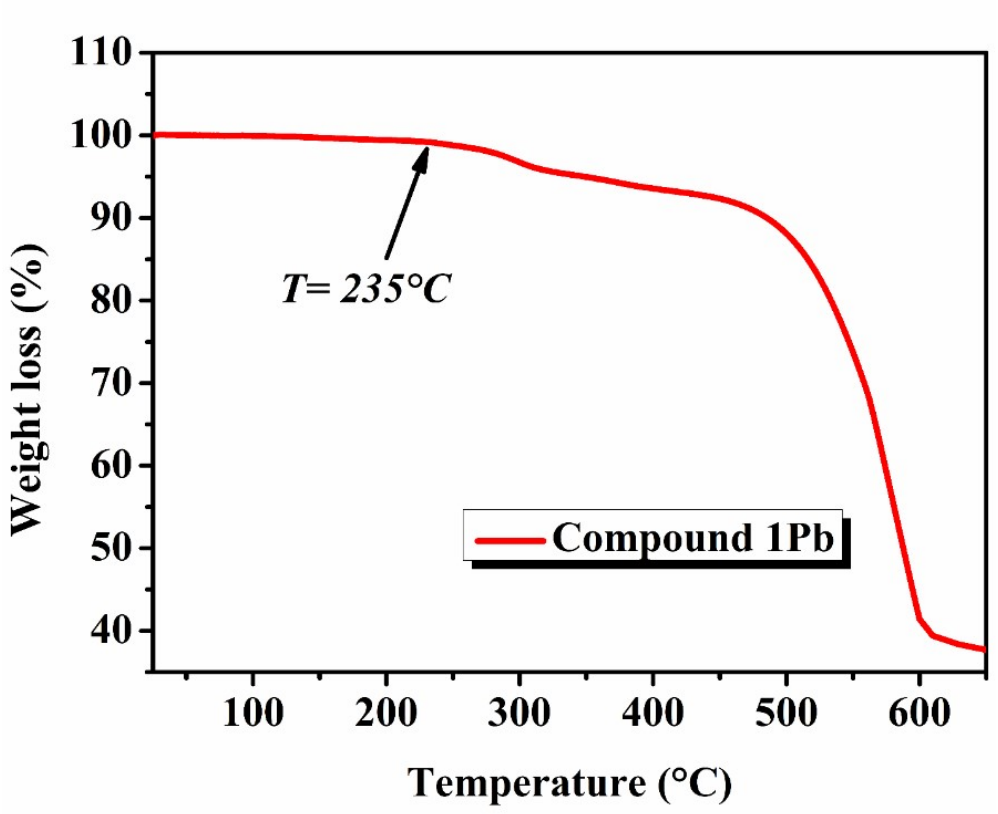

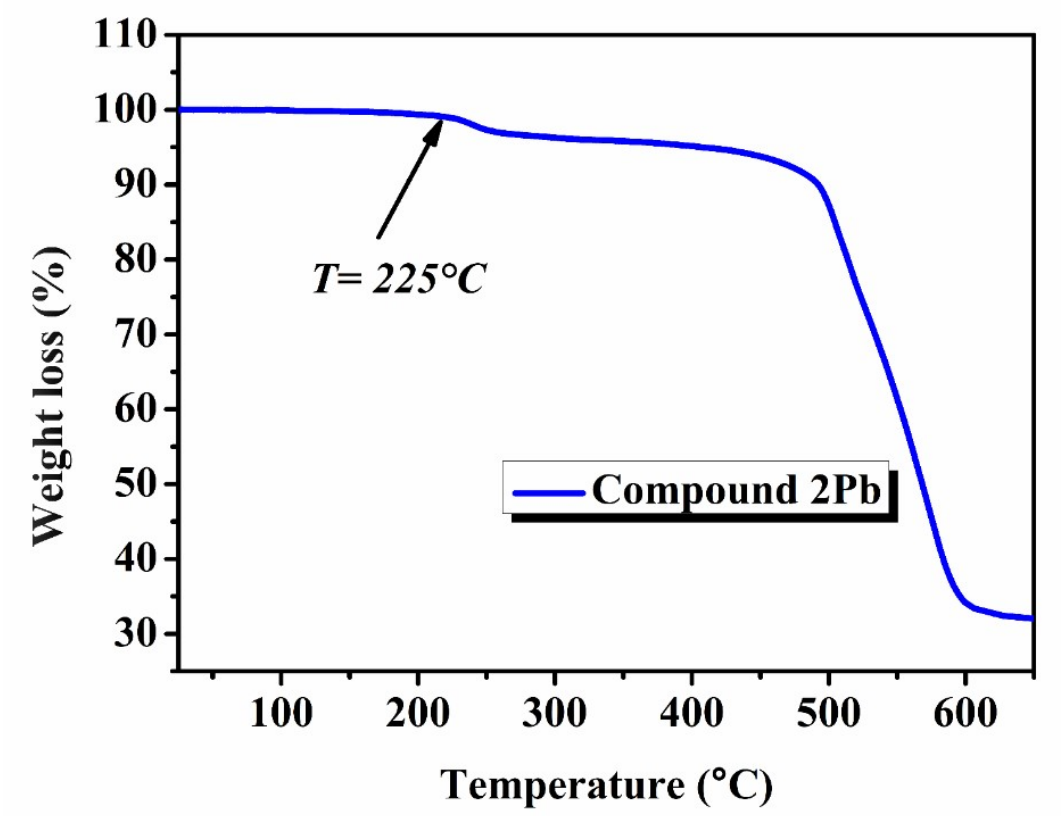

Figure S8. TGA curves of **1Pb** and **2Pb**

References

[1] G. M. Sheldrick, *Acta Crystallogr. A*., ***2008***, 64, 112-122.

[2] O. V. Dolomanov, L. J. Bourhis, R. J. Gildea, J. A. K, Howard, H. Puschmann, OLEX2: A complete structure solution, refinement and analysis program (***2009)***. *J. Appl. Cryst*., 42, 339-341.

[3] G. Kresse and J. Furthmüller, Phys. Rev. B: *Condens. Matter Mater. Phys.*, ***1996***, 54, 11169–11186.

[4] G. Kresse and J. Furthmüller, *Comput. Mater. Sci.*, ***1996***, 6, 15–50.

[5] G. Kresse and D. Joubert, Phys. Rev. B: *Condens. Matter Mater. Phys.*, ***1999***, 59, 1758–1775.

[6] X-Y. Sun, M. Yue, Y-X. Jiang, C-H. Zhao, Y-Y. Liao, X-W. Lei, and C-Y. Yue, Combining Dual-Light Emissions to Achieve Efficient Broadband Yellowish-Green Luminescence in One-Dimensional Hybrid Lead Halides, *Inorg. Chem*. **2021**, *60*, 1491−1498.

[7] C-Q. Jing, J-Z. Li, T. Xu, K. Jiang, X-J. Zhao, Y-F. Wu, N-T. Xue, Z-H. Jing and X-W. Lei, Organic cations directed 1D $[Pb_3Br_{10}]$ 4−chains: syntheses, crystal structures, and photoluminescence properties, *CrystEngComm*, **2021**, *23*, 292-298.

[8] Y. Li, C. Ji, L. Li, S. Wang, S. Han, Y. Peng, S. Zhang and J. Luo, (γ-Methoxy propyl amine)$_2$PbBr$_4$: a novel two-dimensional halide hybrid perovskite with efficient bluish white-light emission, *Inorg. Chem. Front*, **2021**, *8*, 2119-2124.

[9] X-L. Lin, B. Chen, Y-R. Huang, K-Y. Song, P-K. Zhou, L-L. Zong, H-H. Li, Z-R. Chen and R. Jiang, Achievement of intrinsic white light emission by hybridization-deformable haloplumbates with rigid luminescent naphthalene motifs, *Inorg. Chem. Front*, **2020**, *7*, 4477-4487.

[10] J. K. Pious, A. Katre, C. Muthu, S. Chakraborty, S. Krishna, and C. Vijayakumar, Zero-Dimensional Lead-Free Hybrid Perovskite-like Material with a Quantum-Well Structure, *Chem. Mater*., **2019**, *31*, 1941−1945.

[11] L-M. Zhao, W-T. Zhang, K-Y. Song, Q-Q. Wu, Y. Li, H-H. Li and Z-R. Chen, Lead-carboxylate/polyiodide hybrids constructed from halogen bonding and asymmetric

viologen: structures, visible-light-driven photocatalytic properties and enhanced photocurrent responses, *CrystEngComm*., **2018**, *20*, 2245-2252.

[12] A. Dey, J. Ye, A. De, E. Debroye, S. K. Ha, E. Bladt, A. S. Kshirsagar, Z. Wang, J. Yin, Y. Wang, L. N.Quan, F. Yan, M. Gao, X. Li, J. Shamsi, T. Debnath, M. Cao, M. A. Scheel, S. Kumar, J. A. Steele, M. Gerhard, L. Chouhan, K. Xu, X-g. Wu, Y. Li, Y. Zhang, A. Dutta, C. Han, I. Vincon, A. L. Rogach, A. Nag, A. Samanta, B. A. Korgel, C-J. Shih, D. R. Gamelin, D. H. Son, H. Zeng, H. Zhong, H. Sun, H. V. Demir, I. G. Scheblykin, I. M-Seró, J. K. Stolarczyk, J. Z. Zhang, J. Feldmann, J. Hofkens, J. M. Luther, J. P-Prieto, L. Li, L. Manna, M. I. Bodnarchuk, M. V. Kovalenko, M. B. J. Roeffaers, N. Pradhan, O.F. Mohammed, O. M. Bakr, P. Yang, P. M-Buschbaum, P V. Kamat, Q. Bao, Q. Zhang, R. Krahne, R. E. Galian, S. D. Stranks, S. Bals, V. Biju, W. A. Tisdale, Y. Yan, R. L. Z. Hoye, and L. Polavarapu, State of the Art and Prospects for Halide Perovskite Nanocrystals., *ACS Nano*., **2021**, *15*, 10775−10981.

[13] X. Tian, Y. Zhang, R. Zheng, D. Wei, and J. Liu, Two-dimensional organic–inorganic hybrid Ruddlesden–Popper perovskite materials: preparation, enhanced stability, and applications in photodetection, *Sustainable Energy Fuels*., **2020**, *4*, 2087-2113.

[14] D. Ma, R. Wang, J. Zhao, Q. Chen, L. Wu, D. Li, L. Su, X. Jiang, Z. Luo, Y. Ge, J. Li, Y. Zhang and H. Zhang, A self-powered photodetector based on two-dimensional boron nanosheets, *Nanoscale*., **2020**, *12*, 5313-5323.

[15] Y. Tang, M. Liang, Bi. Chang, H. Sun, K. Zheng, T. Pulleritsd and Q. Chi, Lead-free double halide perovskite Cs_3BiBr_6 with well-defined crystal structure and high thermal stability for optoelectronics, *J. Mater. Chem. C*, **2019**, *7*, 3369-3374.

[16] Y. Dang, G. Tong, W. Song, Z. Liu, L. Qiu, L. K. Ono and Y. Qi, Interface engineering strategies towards $Cs_2AgBiBr_6$ single-crystalline photodetectors with good Ohmic contact behaviours, *J. Mater. Chem. C*., **2020**, *8*, 276-284.